Steel and Composite Structures, *Vol. 15, No. 2 (2013) 203-220*
DOI: http://dx.doi.org/10.12989/scs.2013.15.2.203

Stability condition for the evaluation of damage in three-point bending of a laminated composite

Mokaddem Allel*, Alami Mohamed and Boutaous Ahmed

Faculty of Science, Department of Physics, U.S.T.O., BP 1505 Oran, Algeria

(Received May 31, 2012, Revised June 02, 2013, Accepted July 10, 2013)

Abstract. The study of the tensile strength of composite materials is far more complex than analysis of the properties of elasticity and plasticity. Indeed, during mechanical loading, micro-cracks in the matrix, the fibers break, debonding of the interfaces are created. The failure process of composites is of great diversity and cannot be described if even we know: the strength criterion of each individual component, the state of stress and strain in the material, the propagation phenomena cracks in the structure and nature of the interface between the matrix and the reinforcement. This information is only partially known and the obtained by the analysis of a stress limit beyond which there is destruction of the material is almost impossible. To partially process the issue, a solution lies in a mesoscopic approach of seeking a law to locate the ultimate strength of the material for a plane stress state. Tests on rectangular plates in bending PEEK/APC2 and T300/914 three were made and this in order to validate our approach, the calculation has been implemented in a nonlinear finite element code (Castem 2000), in order to make comparison with the numerical results. The results show good agreement between numerical simulation and the two materials; however, it would be interesting to consider other phenomena in the criterion.

Keywords: failure criterion; three-point bending; damage; laminated composite; interface

1. Introduction

Often, the use of various criteria (TSAI-HILL, HASHIN, ...) existing in the literature, all depend on a number of parameters that are precisely ultimate strengths for elementary stresses, unlike the test, a law allows estimate the strength characteristics of the composite, and highlights some aspects of the failure mechanism taking into account the strength characteristics of various components of the material. Hachemane *et al*. (2006), Ladèveze *et al*. (2000), Rosen (1964), Chen *et al*. (2011), Scop and Argon (1964).

The work presented in this article aims, the study of the behavior of composite materials, taking account of their damage during the solicitation and their fracture behavior under monotonic axial loading. A mesoscopic approach end of the continuum mechanics based on the theory of periodic homogenization Boutaous *et al*. (2006), Reese (2003) was adopted and coupled with damage, this damage model was proposed and presented by Allen (2001), Boutaous *et al*. (2006), Reese (2003): to take into account the degradation at the fiber matrix interface.

*Corresponding author, Doctor of Science, E-mail: mokaddem.allel@gmail.com

http://www.techno-press.org/?journal=scs&subpage=8 ISSN: 1229-9367 (Print), 1598-6233 (Online)

2. Reminder on modeling the elementary layer

Damageable elastoplastic model of the elementary layer presented by Blassiau (2005), Blassiau *et al*. (2006), Blassiau *et al*. (2008) is based on models developed by Boutaous *et al*. (2006), Lemaitre (1985) in these models, the formulation of the evolution of damage is implicit since we have.

$$W_e = f(\sigma), \quad Y = g(\sigma, d), \quad or \quad d = l(Y) \quad \text{from where } d = l(d, \sigma)$$

The evolution of damage is formulated explicitly, since we have $d = l(\varepsilon)$, the problem of singularity for "d = 1" no longer arises. Moreover this model written in deformation respects the symmetry matrices of rigidities associated with incremental forms of constitutive equations.

The energy density of elastic deformation which is taken as thermodynamic potential is given by

$$2W_e = \frac{\sigma_{11}^2}{E_{11}} + \frac{\sigma_{22}^2}{E_{22}} - \frac{2\nu_{12}\sigma_{11}\sigma_{22}}{E_{11}} + \frac{\sigma_{12}^2}{E_{12}} + \frac{\sigma_{33}^2}{E_{13}} + \frac{\sigma_{23}^2}{E_{23}} \tag{1}$$

The constraints are expressed in terms of deformation as follows

$$\begin{cases} \sigma_{11} = C_{11}(\varepsilon_{11} + \nu_{21}\varepsilon_{22}) \\ \sigma_{22} = C_{22}(\varepsilon_{22} + \nu_{12}\varepsilon_{11}) \\ \sigma_{12} = G_{12}\gamma_{12}\,, \quad \sigma_{13} = G_{13}\gamma_{13.}\,, \quad \sigma_{23} = G_{23}\gamma_{23} \end{cases} \tag{2}$$

with

$$C_{11} = \frac{E_{11}}{1 - \nu_{12}\nu_{21}}\,, \quad C_{22} = \frac{E_{22}}{1 - \nu_{12}\nu_{21}}$$

Taking into account the relationship of symmetry from the existence of a thermodynamic potential we must have

$$\frac{C_{11}}{C_{22}} = \frac{E_{11}}{E_{22}} = \frac{\nu_{12}}{\nu_{21}}, \quad \text{it comes:} \quad \nu_{21}C11 = \nu_{12}C22.$$

And the following definition C_{11}, we note that

$$C_{11}(1 - \nu_{12}\nu_{21}) = E_{11} \Rightarrow C_{11} = E_{11} + \nu_{12}\nu_{21} = E_{11} + \nu_{12}^2 C_{22}$$

In this form, the stress value $\sigma_{22} = C_{22}(\varepsilon_{22} + \nu_{12}\varepsilon_{11})$ apparatus clearly.
The elastic strain energy can be written now Boutaous *et al*. (2006).

$$\begin{cases} 2W_e = E_{11}\varepsilon_{11}^2 + \nu_{12}^2\varepsilon_{11}^2 + 2\nu_{12}C_{22}\varepsilon_{11}\varepsilon_{22} + C_{22}\varepsilon_{22}^2 + G_{12}\gamma_{12}^2 + G_{13}\gamma_{13}^2 + G_{23}\gamma_{23}^2 \\ \quad\;\; = E_{11}\varepsilon_{11}^2 + C_{22}(\varepsilon_{22} + \nu_{12}\varepsilon_{11})^2 + G_{12}\gamma_{12}^2 + G_{13}\gamma_{13}^2 + G_{23}\gamma_{23}^2 \end{cases}$$

2.1 Damage to the elementary layer

2.1.1 Model assumptions

The model is developed at the meso level based on the characteristics of damage at the micro level, as it was observed that the damage ceremonial form of cracks located in the matrix and arranged parallel to the fibers. More damage is assumed to occur only in transverse shear and tension. Indeed, in transverse compression cracks tend to close, and do not create further damage. Finally in the fiber direction, there is a fall of longitudinal modulus in compression due to localized buckling of the fibers.

At the basic layer, the modules are affected by damage and two variables. The module is affected by a variable "ξ_{11}" translating the loss of stiffness of the fibers in longitudinal compression and the brittle fracture in tension in the direction of fibers Boutaous *et al*. (2006).

He then comes to the elastic moduli of the material

$$\begin{cases} E_{11} = E_{11}^0(1-\xi_{11}) \\ C_{22} = C_{22}^0(1-d_{22}) \quad \text{if} \quad \varepsilon_{22} + \nu_{12}\varepsilon_{11} > 0 \\ C_{22} = C_{22}^0 \quad \text{si} \quad \varepsilon_{22} + \nu_{12}\varepsilon_{11} \le 0 \\ G_{12} = G_{12}^0(1-d_{12}) \end{cases}$$

where the subscript "^{0}" denotes the state of virgin material, and lack of experimental information on other modules they are not supposed to be damaged.

From where

$$\nu_{12} = \nu_{12}^0\,, \quad G_{13} = G_{13}^0\,, \quad G_{23} = G_{23}^0$$

In such a transverse $G_{12}^0 = G_{13}^0$ isotropic material initially may not remain with transverse sotropy $G_{12}^0 \neq G_{13}^0$.

The modulus E_{22} and Poisson's ratio ν_{21} are also affected by the damage. However, d'' is the variable that is affecting E_{22} i.e.

$$E_{22} = E_{22}^0(1-d''),$$

it follows that

$$\nu_{21} = \nu_{12}\frac{E_{22}}{E_{11}} = \nu_{12}^0\frac{E_{22}^0(1-d'')}{E_{11}^0} = \nu_{21}^0(1-d''),$$

d_{22} and d'' are thus linked by the relationship between C_{22} and E_{22} thereby according d_{22} to clarify d''

$$\Rightarrow d_{22} = \frac{d''}{1-\nu_{12}^0\nu_{21}^0(1-d'')}$$

The relative error committed by d'' replacing d_{22} then

$$\frac{d_{22}-d''}{d''} = \frac{\nu_{12}^0\nu_{21}^0(1-d'')}{1-\nu_{12}^0\nu_{21}^0(1-d'')}.$$

It is maximum in [0,1] decreases up to 0 and into $d'' = 1$.

The maximum value is equal to

$\dfrac{\nu_{12}^0\nu_{21}^0}{1-\nu_{12}^0\nu_{21}^0}$ who remains weak as long as: $\nu_{12}^0\nu_{21}^0 \le 1$, what is checked for studied materials

Variables d'' and d_{22} are substantially identical.

2.1.2 Damage to the matrix and fiber matrix interface

The matrix damage by transverse tensile microcracking and degradation suffered by the fiber-matrix interface shear and transverse tension, and finally the nonlinear behavior of fibers in longitudinal compression, weak in tension in the direction of fibers, respectively, are modeled by internal variables D_{12}, D_{22}, δ_{12}, δ_{22}, ξ_{11}.

The matrix

The matrix has a damage behavior both in transverse tensile shear. Two internal variables are defined.

- D_{12} associated with the shear modulus G_{12}^m,
- D_{22} associated with the module cross C_{12}^m.

The energy density of elastic deformation of the matrix can be written

$$2W_e^m = E_{11}^m \varepsilon_{11}^2 + C_{22}^m \langle \varepsilon_{22} + \nu_{12}^m \varepsilon_{11} \rangle_-^2 + C_{22}^m (1 - D_{22}) \langle \varepsilon_{22} + \nu_{12}^m \varepsilon_{11} \rangle_+^2 + G_{12}^m (1 - D_{12}) \gamma_{12}^2 \tag{4}$$

Thermodynamic forces associated with internal variables are calculated as follows

$$\begin{cases} Y_{D_{12}} = -\dfrac{\partial W_e^m}{\partial D_{12}} = \dfrac{1}{2} G_{12}^m \gamma_{12}^2 \\ Y_{D_{22}} = -\dfrac{\partial W_e^m}{\partial D_{12}} = \dfrac{1}{2} C_{22}^m \left\langle \varepsilon_{22} + \nu_{12}^m \varepsilon_{11} \right\rangle_+^2 \end{cases}$$

To study the type of damage, the amount representing the state of stress within the material that seems best suited, is a form of energy release rate $G = G_I + G_{II}$. There is also a coupling between D_{12} and D_{22}. The area of damage cannot be characterized by variable changes $Y_{eq} = \sqrt{Y_{D_{12}} + bY_{D_{22}}}$.

The criterion function “*g*” Defining the scope of no damage is then given by

$$g(Y_{eq}, e) = Y_{eq} - e \quad with: \quad e \quad \text{the function threshold}$$

Supplementary laws as part of standard models are written

$$\begin{cases} \dot{D}_{12} = \dot{\lambda}_D \dfrac{\partial g}{\partial Y_{D_{12}}} = \dfrac{1}{2Y_{eq}} \dot{\lambda}_D \\ \dot{D}_{22} = \dot{\lambda}_D \dfrac{\partial g}{\partial Y_{D_{22}}} = \dfrac{1}{2Y_{eq}} \dot{\lambda}_D. \end{cases}$$

And the evolution laws of damage of the matrix are given by

$$\begin{cases} D_{12} = f_m(\underline{Y_{eq}}) \\ D_{22} = bf_m(\underline{Y_{eq}}) \quad with \quad \underline{Y_{eq}} = sup_{\tau \le t} Y_{eq}. \end{cases}$$

where “sup” reflects the irreversibility of the damage.

The fiber-matrix interface

The interface has a behavior

- damageable elastic shear,
- transverse tensile elastic brittle.

Two new internal damage variables are introduced.

- associated shear,
- associated with the transverse traction

The interface is a zone of very thin with a stiff spring type where everything happens as if there was a moving surface discontinuity $(\sigma\vec{n} = f([|u|]))$.

Normal and tangential stresses in the fiber direction are related to jumps of displacements between the two circles by a linear elastic law

$$\begin{cases} |u|_{\vec{x}_1} = \dfrac{\sigma_{12}}{k_{66}} \\ |u|_{\vec{x}_2} = \dfrac{\langle\sigma_{22}\rangle_+}{k_{22}} \end{cases}$$

k_{22} whether or k_{66} tend to infinity, the interface is perfect.

with: k_{ii} the terms of the tangent stiffness.

If damage is taken into account, the law is written

$$\begin{cases} |u|_{\vec{x}_1} = \dfrac{\sigma_{12}}{k_{66}(1-\delta_{12})} \\ |u|_{\vec{x}_2} = \dfrac{\langle\sigma_{22}\rangle_+}{k_{22}(1-\delta_{22})}. \end{cases}$$

The elastic energy density of the interface is taken as damaged thermodynamic potential and in the form

$$2E_i = k_{66}(1-\delta_{12})\gamma_{12}^2 + k_{22}(1-\delta_{22})\langle\varepsilon_{22}\rangle_+^2.$$

Associated variables are defined by

$$\begin{cases} Y_{\delta_{12}} = -\dfrac{\partial E_i}{\partial \delta_{12}} = \dfrac{1}{2}k_{66}\gamma_{12}^2 \\ Y_{\delta_{22}} = -\dfrac{\partial E_i}{\partial \delta_{22}} = \dfrac{1}{2}k_{22}\langle\varepsilon_{22}\rangle_+^2. \end{cases}$$

As with the matrix, complementary laws are written

$$\begin{cases} \dot{\delta}_{12} = \dot{\lambda}_\delta \dfrac{\partial g}{\partial Y_{\delta_{12}}} \\ \dot{\delta}_{22} = \dot{\lambda}_\delta \dfrac{\partial g}{\partial Y_{\delta_{22}}}. \end{cases}$$

And the evolution laws are given by

$$\begin{cases} \delta_{12} & = f_i(\underline{Y_{\delta_{12}}}) \\ \delta_{22} & = h(\underline{Y_{\delta_{22}}}) \end{cases} \quad h \quad \text{function of Heavyside}$$

with

$$\begin{cases} \underline{Y_{\delta_{12}}} & = sup_{\tau \le t} Y_{\delta_{12}} \\ \underline{Y_{\delta_{22}}} & = sup_{\tau \le t} Y_{\delta_{22}}. \end{cases}$$

2.1.3 Homogenization of the elementary layer

The calculation of homogenization is carried out on modules E_{22} and G_{12}. The method of asymptotic expansions for periodic media is used by Altuni ik *et al*. (2010), Phoenix and Beyerlein (2000), Rosen (1964). By designating d_{12} and d_{22} loss of rigidity of the layer it comes Van den Heuvel *et al*. (1998)

$$\begin{cases} \dfrac{1}{G_{12}(1-d_{12})} = \dfrac{v_m}{G_{12}^m(1-D_{12})} + \dfrac{2}{k_{66}(1-\delta_{12})} \\ \dfrac{1}{E_{22}(1-d_{22})} = \dfrac{v_m}{E_{22}^m(1-D_{22})} + \dfrac{1}{k_{22}(1-\delta_{22})}. \end{cases}$$

With v_m: the volume fraction of matrix.

By performing an expansion near the "0" damage of the layer are then given by

$$\begin{cases} d_{12} = \dfrac{v_m G_{12} D_{12}}{G_{12}^m} + \dfrac{2G_{12}\delta_{12}}{k_{66}} \\ d_{22} = \dfrac{v_m E_{22} D_{22}}{E_{22}^m} + \dfrac{E_{22}\delta_{22}}{k_{22}} \end{cases}$$

For a relatively simple model and consistent with that developed by Herakovitch *et al*. (2000), to take the damage of the layer as a sum of elemental damage due respectively to the matrix and the fiber-matrix interface.

2.1.4 Model of damage

In the mesoscale model, there are only three internal variables: two variables and damage, d_{12} and d_{22} a variable "ξ_{11}" reflecting the loss of stiffness of the fibers in compression.

Damageable elastic law reads

$$\begin{cases} \sigma_{11} & = E_{11}^0(1-\xi_{11})\varepsilon_{11}^e + (\nu_{12}^0)^2 C_{22}^0(1-d_{22})\varepsilon_{11}^e + \nu_{12}^0 C_{22}^0(1-d_{22})\varepsilon_{22}^e \\ \sigma_{22} & = \nu_{12}^0 C_{22}^0(1-d_{22})\varepsilon_{11}^e + C_{22}^0(1-d_{22})\varepsilon_{22}^e \\ \sigma_{12} & = G_{12}^0(1-d_{12})\gamma_{12}^e \end{cases} \tag{5}$$

3. Nonlinear strain energy

3.1 Nonlinear strain tensors

Rupture of the elementary layer results in a condition of instability of the tangential behavior. For this, we must derive the elastic damageable law and the law and obtain incremental. The failure criterion is reached when the determinant of matrix incremental changes sign (becomes singular).

It is possible to give a more physical approach, specifying that it when there's instability pageantry up on the stress-strain curve, For the failure criterion, we must calculate the instability condition given by

$$det_{\dot{\sigma}\to\infty}(K_{tg}) = 0.$$

So, Given

$$\left|\begin{array}{l} \nu_{12} = \nu_{12}^{0} \\ C_{22} = C_{22}^{0}(1-d_{22}) \\ G_{12} = G_{12}^{0}(1-d_{12}) \end{array}\right.$$

We can write the model as follows

$$\begin{cases} \sigma_{11} & = C_{11}\varepsilon_{11} + \nu_{12}C_{22}\varepsilon_{22} = (E_{11} + \nu_{12}C_{22})\varepsilon_{11} + \nu_{12}C_{22}\varepsilon_{22} \\ \sigma_{22} & = C_{22}\varepsilon_{22} + \nu_{12}C_{22}\varepsilon_{11} \\ \sigma_{12} & = G_{12}\gamma_{12} \end{cases} \tag{6}$$

Associated incremental law is in the form

$$\begin{cases} \dot{\sigma}_{11} = (E_{11} + (\nu_{12}^{0})^{2}C_{22})\dot{\varepsilon}_{11} + \nu_{12}^{0}C_{22}\dot{\varepsilon}_{22} + \dot{\tau}_{11} \\ \dot{\sigma}_{22} = C_{22}\dot{\varepsilon}_{22} + \nu_{12}^{0}C_{22}\dot{\varepsilon}_{11} + \dot{\tau}_{22} \\ \dot{\sigma}_{12} = G_{12}\dot{\gamma}_{12}\dot{\tau}_{12} \end{cases} \tag{7}$$

with

ε_{11}^{c} denotes the longitudinal strain at rupture compression, and γ being the loss of stiffness in longitudinal compression that is given by

$$\text{in the longitudinal direction} \quad \xi_{11} = \begin{cases} 0 & si \quad \varepsilon_{11} > 0 \quad and \quad \chi_f = 0 \\ -\gamma\varepsilon_{11} & si \quad \varepsilon_{11} < 0 \quad and \quad \chi_f = 0 \\ 1 & si \quad \chi_f = 0. \end{cases}$$

The model integrates itself the different failure criteria. Interface with brittle behavior in tension transverse, it is natural to introduce an indicator of rupture as

$\chi_i = 0$ until there is no break, i.e., as $Y'_i < Y'_r$,

if $Y'_i \geq Y'_r$ then $\chi_i = 1$.

Similarly to the rupture of the transverse matrix compression, if the criterion is verified Hashin matrix breaks, which leads to define "χ_μ", indicator of the breakdown of the matrix, as follows

$\chi_\mu = 0$ until there is no break, i.e., as long as $\mu < 1$, if $\mu \geq 1$ then $\chi_\mu = 1$.

Finally, for the fiber breakage criterion selected is a different criterion of maximum deformation in tension and compression, either

"$\chi_f = 0$" as there is no break, i.e., as long as $\varepsilon_{11}^{c} < \varepsilon_{11} < \varepsilon_{11}^{t}$,

if $\varepsilon_{11} \geq \varepsilon_{11}^{t}$ or $\varepsilon_{11} \geq \varepsilon_{11}^{c}$ then $\chi_f = 1$, where ε_{11}^{t} and ε_{11}^{c} denote the longitudinal strains at failure in tension and compression.

However

$$\begin{cases} \dot{\xi}_{11} = -\gamma\dot{\varepsilon}_{11}H(-\varepsilon_{11})H(\varepsilon_{11} - \varepsilon_{11}^{c}) \\ \dot{d}_{22} = \dot{\tau}^{'}(1-\chi_i)H(1-z^{'})H(1-z)H(\sigma_{22}) \\ \dot{d}_{12} = \dot{\tau}(1-\chi_i)H(1-z^{'})H(1-z) \end{cases} \tag{9}$$

and

$$\left| \begin{array}{l} \dot{\tau} = \dfrac{H(Y_m - Y_0)}{bY_c}\dot{Y}_m + \dfrac{H(Y_i - Y_0^{'})}{Y_c^{'}}\dot{Y}_i^{'} \\ \dot{\tau}^{'} = \dfrac{H(Y_m - Y_0)}{Y_c}\dot{Y}_m \end{array} \right. \tag{10}$$

we put

$$\left| \begin{array}{l} B = \dfrac{H(Y_m - Y_0)H(\dot{Y}_m)}{2Y_cY_m} \\ C = \dfrac{H(Y_i - Y_0^{'})H(\dot{Y}_i)}{2Y_c^{'}Y_i} \end{array} \right.$$

The thermodynamic variables associated with internal variables are defined by

$$\begin{cases} Y_{12} = -\dfrac{\partial W_e}{\partial d_{12}} = \dfrac{1}{2}G_{12}^{0}\gamma_{12}^{2} \\ Y_{22} = -\dfrac{\partial W_e}{\partial d_{22}} = \dfrac{1}{2}C_{22}^{0}\langle \varepsilon_{22} + \nu_{12}^{0}\varepsilon_{11} \rangle_{+}^{2}. \end{cases}$$

Variables and thresholds defining the areas of damage are not given by

$$\begin{cases} Y_m = sup_{\tau \leq t}\sqrt{Y_{12} + bY_{22}} \leftarrow \text{damage of the matrix} \\ Y_i = sup_{\tau \leq t}\sqrt{Y_{12}} \leftarrow \text{damage of the interface in shearing} \\ Y_i^{'} = sup_{\tau \leq t}\sqrt{Y_{22}} \leftarrow \text{damage of the interface between transverse action} \\ \mu = [\dfrac{\langle \sigma_{22} \rangle_{-}}{\sigma_{22}^{c}}((\dfrac{\sigma_{22}}{2\sigma_{12}^{r}})^2 - 1]] + (\dfrac{< \sigma_{22} >_{-}}{2\sigma_{12}^{r}})^2 + (\dfrac{\sigma_{12}}{\sigma_{12}^{r}})^2 : \text{criterion of Hasine:} \\ \text{stamp in compression} \end{cases}$$

with

- initial threshold of damage to the matrix,
- initial threshold of damage to the interface,
- strength of the matrix,
- resistance of the interface transverse tensile,
- resistance of the interface shear,
- loss of stiffness in longitudinal compression,
- coupling coefficient that quantifies the relative influence and material degradation

$$\text{from which}(10) \Leftrightarrow \left| \begin{array}{l} \dot{\tau} = \dfrac{B}{b}[\widetilde{\sigma}_{12}\dot{\gamma}_{12} + b\langle\widetilde{\sigma}_{22}\rangle_{+}(\dot{\varepsilon}_{22} + \nu_{12}^{0}\dot{\varepsilon}_{11})] + A\widetilde{\sigma}_{12}\dot{\gamma}_{12} \\ \dot{\tau}' = B[\widetilde{\sigma}_{12}\dot{\gamma}_{12} + b\langle\widetilde{\sigma}_{22}\rangle_{+}(\dot{\varepsilon}_{22} + \nu_{12}^{0}\dot{\varepsilon}_{11})] \end{array} \right.$$

We put: $F = (1-\chi_i)H(1-z)H(1-z')$

$$\text{from which}(9) \Leftrightarrow \begin{cases} \dot{\xi}_{11} = -\gamma\dot{\varepsilon}_{11}H(-\varepsilon_{11})H(\varepsilon_{11} - \varepsilon_{11}^{c}) \\ \dot{d}_{22} = FH(\sigma_{22})B[\widetilde{\sigma}_{12}\dot{\gamma}_{12} + b\langle\widetilde{\sigma}_{22}\rangle_{+}(\dot{\varepsilon}_{22} + \nu_{12}^{0}\dot{\varepsilon}_{11})] \\ \dot{d}_{12} = \dfrac{FB}{b}[\widetilde{\sigma}_{12}\dot{\gamma}_{12} + b\langle\widetilde{\sigma}_{22}\rangle_{+}(\dot{\varepsilon}_{22} + \nu_{12}^{0}\dot{\varepsilon}_{11})] + FA\widetilde{\sigma}_{12}\dot{\gamma}_{12} \end{cases}$$

It is therefore obtained

$$(8) \Leftrightarrow \begin{bmatrix} \dot{\tau}_{11} \\ \dot{\tau}_{22} \\ \dot{\tau}_{12} \end{bmatrix} = \begin{bmatrix} T & -bBFH(\widetilde{\sigma}_{22})\nu_{12}^{0}\langle\widetilde{\sigma}_{22}\rangle_{-}^{2} & -FB\nu_{12}^{0}\langle\widetilde{\sigma}_{22}\rangle_{-}\widetilde{\sigma}_{12} \\ -bBFH(\widetilde{\sigma}_{22})\nu_{12}^{0}\langle\widetilde{\sigma}_{22}\rangle_{-}^{2} & -bBFH(\widetilde{\sigma}_{22})\langle\widetilde{\sigma}_{22}\rangle_{-}^{2} & -FB\langle\widetilde{\sigma}_{22}\rangle\widetilde{\sigma}_{12} \\ -FB\nu_{12}^{0}\langle\widetilde{\sigma}_{22}\rangle\widetilde{\sigma}_{12} & -FB\langle\widetilde{\sigma}_{22}\rangle_{-}\widetilde{\sigma}_{12} & -F(A + \dfrac{B}{b})\widetilde{\sigma}_{12}^{2} \end{bmatrix}$$

with

$$T = \widetilde{\sigma}_{11}\gamma H(-\varepsilon)_{11}H(\varepsilon_{11} - \varepsilon_{11}^{c}) - (\nu_{12}^{0})^{2}\langle\widetilde{\sigma}_{22}\rangle_{-}^{2}bBFH(\widetilde{\sigma}_{22})$$

we put

$$\left| \begin{array}{l} P = bBF \\ Q = BF \qquad \Rightarrow (2) \Leftrightarrow \dot{\sigma} = K_{tg}\dot{\varepsilon} \\ R = F(A + \dfrac{B}{b}) \end{array} \right.$$

with

$$K_{tg} = \begin{bmatrix} E_{11} + (\nu_{12}^{0})^{2}C_{22} + T & \nu_{12}^{0}C_{22} - P\nu_{12}^{0}\langle\widetilde{\sigma}_{22}\rangle_{+}^{2} & -Q\nu_{12}^{0}\langle\widetilde{\sigma}_{22}\rangle_{+}\widetilde{\sigma}_{22} \\ \nu_{12}^{0}C_{22} - P\nu_{12}^{0}\langle\widetilde{\sigma}_{22}\rangle_{+}^{2} & C_{22} - P\langle\widetilde{\sigma}_{22}\rangle_{+}^{2} & -Q\langle\widetilde{\sigma}_{22}\rangle_{+}\widetilde{\sigma}_{12} \\ -Q\nu_{12}^{0}\langle\widetilde{\sigma}_{22}\rangle_{+}\widetilde{\sigma}_{12} & -Q\langle\widetilde{\sigma}_{22}\rangle_{+}\widetilde{\sigma}_{12} & G_{12} - R\widetilde{\sigma}_{12}^{2} \end{bmatrix}$$

with: K_{tg} the tangent matrix behavior.

For the failure criterion must therefore calculate the condition of instability.

$$det_{\dot{\sigma}\to\infty}(K_{tg}) = 0$$

Finally after calculation we get

$$\left\| \begin{array}{l} P\dfrac{\langle\tilde{\sigma}_{22}\rangle_+^2}{C_{22}} + R\dfrac{\tilde{\sigma}_{12}^2}{G_{12}} + (Q - RP)\dfrac{\langle\tilde{\sigma}_{22}\rangle_+^2 + \tilde{\sigma}_{12}^2}{G_{12}C_{22}} = 1 \\ or \quad E_{11} + \tilde{\sigma}_{11}\gamma H(-\varepsilon_{11})H(\varepsilon_{11} - \varepsilon_{11}^c) = 0 \end{array} \right.$$

4. Test plates T300 and Peek subject to a three-point bending

Six plates in this paragraph will be presented. Three are made of carbon fiber and epoxy resin Yasmin *et al*. (2003, 2006), Yasmin and Daniel (2004), they are denoted T300. the other three plates are made Peek/APC2 and will be called Peek. For each of these three types of stacking materials are studied. These three stacking sequences differ by the position occupied by the folds in the bedding. All these stacks are symmetric in the thickness and consist of eight elementary folds. These six plates are subject to a three-point bending (Fig. 1).

The geometric characteristics of each material and each empliment sequence are shown above Allel *et al*. (2012).

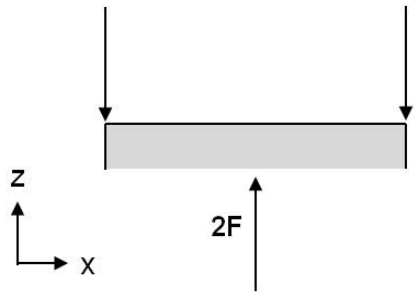

Fig. 1 Plate 3-point bending

1 – T300

Stacking	Thickness	Width	Length	Distance between supports
[0/90/+45/–45]	0.001 m	0.01 m	0.04 m	80 mm
[90/0/+45/–45]	0.001 m	0.01 m	0.025 m	50 mm
[90/+45/0/–45]	0.001 m	0.01 m	0.025 m	50 mm

2 – Peek

Stacking	Thickness	Width	Length	Distance between supports
[0/90/+45/–45]	0.00108 m	0.01 m	0.04 m	80 mm
[90/0/+45/–45]	0.00108 m	0.01 m	0.04 m	50 mm
[90/+45/0/–45]	0.00108 m	0.01 m	0.04 m	50 mm

4.1 Analysis of results for each stack

4.1.1 [0/90/+45/–45] in T300

All phenomena developing in the plate element are initialized in the center and they spread gradually towards the ends.

If only the damage without compression of the fibers is taken into account, the results are identical to those of elasticity.

The analysis of the values of damage variables can note that the shear damage d_{12} is negligible, and it occurs mainly in the layer 45? The transverse tensile damage is also very low before the rupture of the matrix in the layer 90? However, the loss of stiffness appearing in the layer 0? and due to the nonlinearity of the fibers in compression is more important than both damage and is not negligible. The evolution of these three variables is presented in Fig. 2.

4.1.2 [90/0/+45/–45]$_s$ in T300

All phenomena occur in the first element in the center of the plate.

This suggests that in this case, damages are not negligible. However, analysis of changes in the various degradations (Fig. 3) show that they are very low until he breaks the ceremonial fiber-matrix interfaces in the layer 90? The fiber breaks occur only around 220 N and always in the

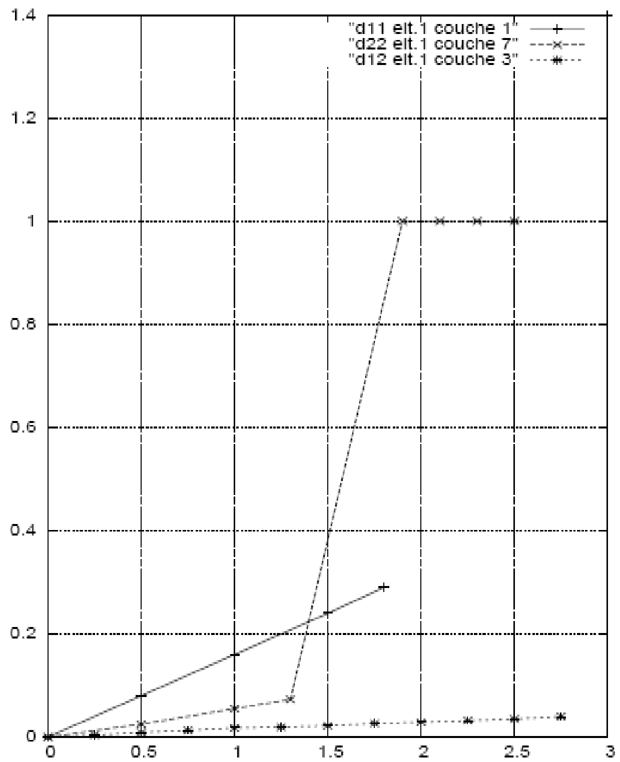

Fig. 2 T300 plate in 3-point bending; damages

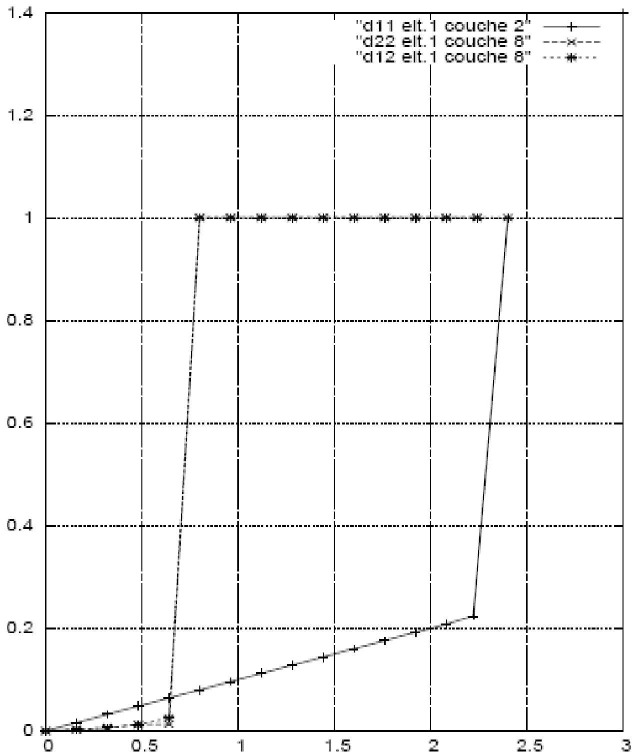

Fig. 3 T300 plate in 3-point bending; damages

layer 0? Experimentally, the breakdown takes place around 238 N. In this case, the calculation is well aware of reality as the final fracture of the plate is detected to 240 N when there are breaks in the matrix transverse compression in the layer 90?, which in this test is on outer portions of the plate.

It seems that for this stack, the damage models are well aware of the actual behavior of the structure.

4.1.3 [90/+45/0/–45]$_s$ in T300

Note also that ceremonial fiber-matrix debonding in the layers 90? and 45? hence the results of damage d_{12} and d_{22} in Fig. 4. Indeed, the damage reaches the maximum value of “1” for relatively low loads. In this case the damage is predominant in the overall behavior of the plate. This plate behaves essentially elastically damageable. For this case, the calculations are realistic, however, the final failure is detected too late.

4.1.4 [0/90/+45/–45]$_s$ Peek

In this plate element, the most sought is located once again at full center. The damage model gives similar results to those obtained if only the behavior of fibers is modeled. These two behaviors are somewhat more flexible and above all close to experimental results.

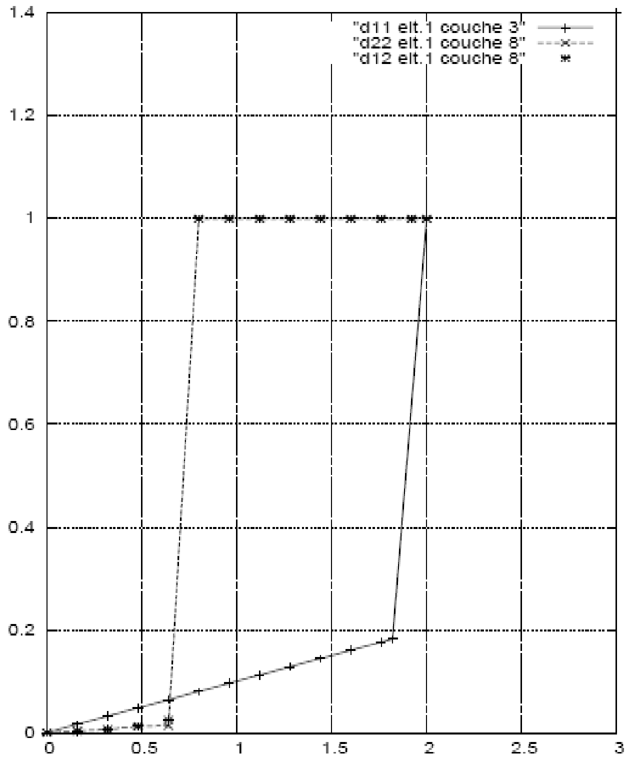

Fig. 4 T300 plate in 3-point bending; damages

It seems that for this stack and the behavior of this material is predominant fibers and damage is negligible. This is confirmed by the analysis of damage curves shown in Fig. 5, where one can note that both types of damage are almost identical and that they reach very low values. This break is given by the rupture of the fibers in the layers 0? which are on the external faces of the plate.

It seems legitimate to say that this plate has an almost elastic nonlinear behavior that appears to be characteristic brittle layers 0? to being in outer skins.

4.1.5 [90/0/+45/–45]$_s$ Peek

In this plate, it begins at the center of the plate and spread to the extremities. For this type of stack, the full damage model gives similar behavior. However they differ when disruptions occur fiber-matrix interface in layers 90? behaviors obtained are too soft. In this case, the breaks are detected too soon as they appear in the calculation to 300 N (due to rupture of the matrix transverse compression in the layer 90?).

In this case, the degradation is negligible as can be seen on the Fig. 6. The transverse damage seems most important.

4.1.6 [90/+45/0/–45]$_s$ Peek

Models taking into account the various degradations have similar behavior until it becomes

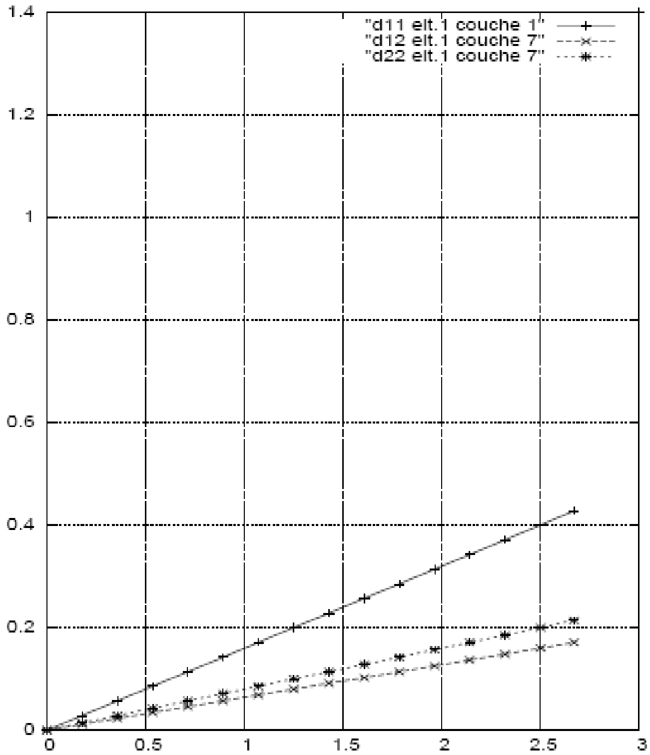

Fig. 5 Plate Peek in 3-point bending; damages

apparent disruptions of fiber-matrix interface in the layer 90?

The damage in transverse shear and tensile are comparable and not significant before they reach the maximum value as a result of breaks as can be noted in Fig. 7.

It seems that this plate has an elastic damageable behavior and that the calculations made with the degradation models adequately reflect the actual behavior of the plate in bending.

5. Comparison between the two materials

In all cases tested for the same piles, the Peek is stronger than the T300 as their final failure occurs at high load levels. Hachemane *et al*. (2006).

For all the stacks and the two materials, it was found that the results are virtually identical to those with the damage model alone.

Regardless of the material or the stacking sequence, all phenomena that occur in these plates, are initialized at the center of the plate and then spread to the ends of the plate.

For the stacking sequence $[0/90/+45/–45]_s$, calculations simulating different models give similar results for both materials processed. Indeed, in both cases, it is the fibers that are predominant and essentially governing the behavior overall plate.

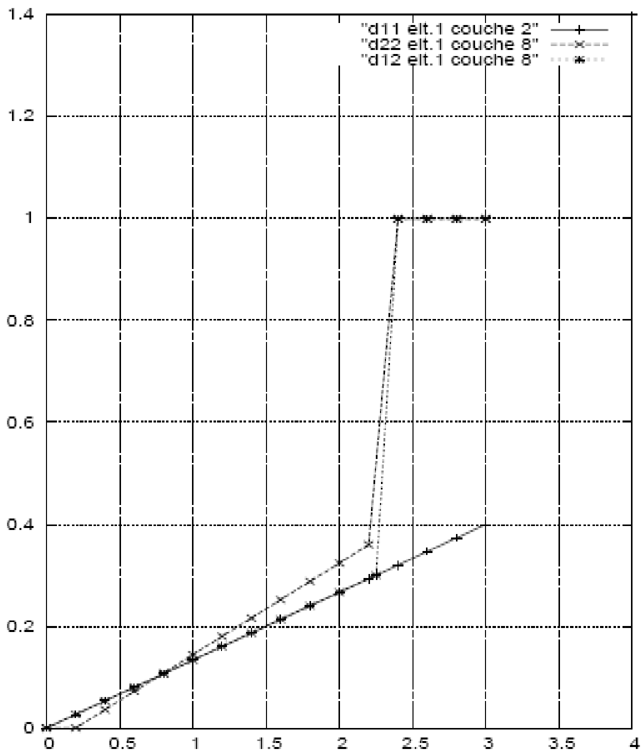

Fig. 6 Plate Peek in 3-point bending; damages

For the stacking sequence [90/0/+45/–45]$_s$ was similar behavior for both materials although at higher charge levels for Peek. In this case, these are the models with damage that best reflect the actual behavior of these plates. In addition, the breaks that appear for the two materials are similar but different loads.

For the stacking sequence [90/+45/0/–45]$_s$, both materials exhibit the same behavior patterns and ruptures are similar in terms of quality.

6. Comparison of results following the stacking sequence

6.1 T300

For all the stacks, the degradation occurring in the first place in the center of the plates and then progressing toward the ends of these plates.

For the stack where the crease 0? is in the outer skin are the fibers that are dominant, while the laminate whose fold 0? is the innermost behavior is essentially a damageable. Finally, the plate having the fold in a second position where all behavior modeled degradations has a significant influence.

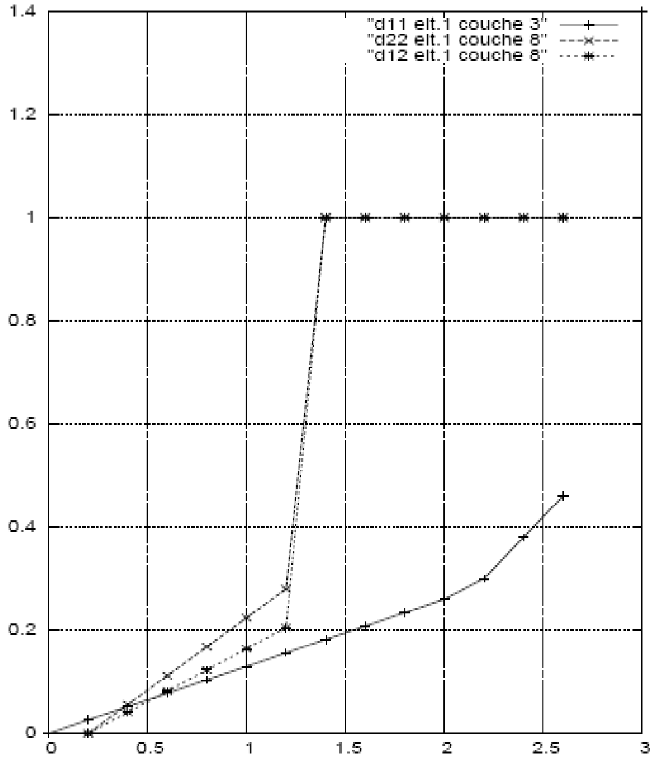

Fig. 7 Plate Peek in 3-point bending; damages

The more resistant plate is the one with the stacking sequence with the 0? outside fold.

6.2 PEEK

The plate with the fold on the 0? outside has a behavior that is governed by the behavior of fibers. This is the stack with the more rigid behavior. its break is given by fiber breakage in layers 0?

For the stacking sequence with the fold 0? at the second position, behaviors obtained numerically are more flexible than in reality. The behavior of this plate is rather damageable.

Finally, the stack where the fold 0? is inside has a behavior that takes into account all the phenomena of degradation modeled.

Based on these observations, the position of the fold in a stack has an important influence on the behavior of the structure.

Finally, in light of these results, the Peek is a stronger material than the T300 as it breaks for higher load levels. It is also a more rigid material because for a given load level gives lower distortion.

The study carried out on plates T300 and Peek with different stacking sequences depending on the position of the fold 0? to the stratification, shows that the Peek is stronger than the T300. The numerical results are behaving fairly close to reality. It was found that depending on the position of the fold in 0? the plates do not have the same behavior.

Indeed, the laminates where the folds are 0? outer behaves essentially as the fibers resiliently i.e., non-linear, whereas the other stacks have an elastic behavior rather damageable.

It therefore appears that the stacking sequence is a factor in optimizing essential calculating laminated composite structures.

7. Conclusions

For validation of plasticity models the results are very satisfactory, since it is observed that different simulated stacks reflect behavior very similar to experimental results.

For the plate in the form of a specimen, the model that best accounts for the actual behavior is that which models all types of degradation coupled to the kinematic plasticity non-linear hardening. Two meshes have been studied for that structure and it was found that in uniaxial tension the mesh has practically no influence on behavior. It is therefore not penalizing the perform calculations on crude meshes.

For plates formed by the superposition of folds at 0° and 90°, it was noted that the overall behavior is essentially dictated by the behavior of the fold at 0°. Moreover, the fact of the composite symmetrical in its thickness increases its resistance.

The study performed on plates with T300 and Peek different stacking sequences depending on the position of the fold at 0° in the stratification, shows that the Peek is stronger than T300. Numerical results show behavior that is quite close to reality. It was found that the position of the fold at 0° plates do not have the same behavior.

Indeed, the laminates where the folds at 0° external skins are essentially behave as fibers i.e., elasic and non-linear, whereas the other stacks have an elastic behavior rather damageable.

References

Allen, D.H. (2001), “Homogenization principles and their application to continuum damage mechanics”, *Compos. Sci. Tech.*, **67**(15), 2223-2230.

Altuni ik, A.C., Bayraktar, A., Sevm, B., Kartal, M.E. and Adanur, S. (2010), “Finite element model updating of an arch type steel laboratory bridge model using semi-rigid connection”, *Steel Compos. Struct. Int. J.*, **10**(6), 541-561.

Blassiau, S. (2005), “Modelling of microstructural phenomena in a unidirectional composite carbon / epoxy and lifetime prediction: Characterization and control of wound tanks”, Ph.D. Thesis, Ecole des Mines de Paris.

Blassiau, S., Thionet, A. and Bunsell, A.R. (2006), “Micromechanisms of load transfert in a unidirectional carbon-fibre epoxy composite due to fibre failures. part 1 : Micromechanisms and 3d analysis of load transfert, the elastic case”, *Compos. Struct.*, **74**(3), 303-318.

Blassiau, S., Thionet, A. and Bunsell, A.R. (2008), “Micromechanisms of load transfert in a unidirectional carbon-fibre epoxy composite due to fibre failures. part 3 : Multiscale reconstruction of composite behaviour”, *Compos. Struct.*, **83**(3), 312-323.

Boutaous, A., Peseux, B., Gornet, L. and Bélaidi, A. (2006), “A new modeling of plasticity coupled with the damage and identification for carbon fibre composites laminates”, *Compos. Struct.*, **74**(1), 1-9.

Chen, S.M., Shi, X.Y. and Qiu, Z.H. (2011), “Shear bond failure in composite slabs– a detailed experimental study”, *Steel Compos. Struct. Int. J.*, **11**(3), 233-250.

Hachemane, B., Mir, A. and Bezzazi, B. (2006) “Elaboration et caractérisation d’un matériaux composites hybride”, *Matéraiux*, 13-17, Dijon France.

Herakovich, C.T., Schroedter III, R.D., Gasser, A. and Guitard, L. (2000), “Damage evolution in $[\pm 45]_s$ laminates with fiber rotation”, *Compos. Sci. Tech.*, **60**(15), 2781-2789.

Ladèveze, P., Allix, O., Deü, J.F. and Lévêque, D. (2000), “A mesomodel for localisation an damage computation in laminates”, *Comput. Method. Appl. Mech. Eng.*, **183**(1-2), 105-122.

Lemaitre, J. (1985), “Coupled elastoplasticity and damage constitutive equations”, *Comput. Method. Appl. Mech. Eng.*, **51**(1-3), 31-49.

Landis, C.M., Beyerlein, I.J. and McMeeking, R.M. (2000), “Micromechanical simulation of the failure of fiber reinforced composites”, *J. Mech. Phys. Solid.*, **48**(3), 621-648.

Mokaddem, A., Alam, M. and Boutaous, A. (2012), “A study by a genetic algorithm for optimizing the arrangement of the fibers on the damage to the fiber–matrix interface of a composite material”, *J. Text. I.*, **103**(12), 1376-1382.

Phoenix, S.L. and Beyerlein, I.J. (2000), “1.19 – Statistical strength theory for fibrous composite materials”, *Compr. Compos. Mater.*, 559-639.

Reese, S. (2003), “Meso-macro modeling of fiber-reinforced rubber-like composites exhibiting large elastoplastic deformation”, *Int. J. S lid. Struct.*, **40**(4), 951-980.

Rosen, B.W. (1964), “Tensile failure of fibrous composites”, *AIAA J.*, **2**(11), 1985-1991.

Scop, P.M. and Argon, A.S. (1969), “Statistical theory of strength of laminated composites II”, *J. Compos. Mater.*, **3**(1), 30-47.

Van den Heuvel, P.W.J., Wubbolts, M.K., Young, R.J. and Peijs, T. (1998), “Failure phenomena in two-dimensional multi-fibre model composites: 5. A finite element study”, *Compos. Part A: Appl. Sci. Manuf.*, **29**(9-10), 1121-1135.

Yasmin, A., Abot, J.L. and Daniel, I.M. (2003), “Characterization of structure and mechanical behavior of clay/epoxy nanocomposites”, Proceedings of the 14th International Conference on Composite Materials, San Diego, CA, USA, July.

Yasmin, A. and Daniel, I.M. (2004), “Mechanical and thermal properties of graphite platelet/epoxy composites”, *Polymer*, **45**(24), 8211-8219.

Yasmin, A., Luo, J.J. and Daniel, I.M. (2006), “Processing of expanded graphite reinforced polymer nanocomposites”, *Compos. Sci. Tech.*, **66**(9), 1182-1189.

CC